

# A single-crystal neutron diffraction study on magnetic structure of the quasi-one-dimensional antiferromagnet $\text{SrCo}_2\text{V}_2\text{O}_8$

Juanjuan Liu,<sup>1</sup> Jinchen Wang,<sup>1</sup> Wei Luo,<sup>1</sup> Jieming Sheng,<sup>1</sup> Zhangzhen He,<sup>2</sup> S.A. Danilkin,<sup>3</sup> and Wei Bao<sup>1\*</sup>

<sup>1</sup>*Department of Physics, Renmin University of China, Beijing 100872, China*

<sup>2</sup>*State Key Laboratory of Structural Chemistry, Fujian Institute of Research on the Structure of Matter, Chinese Academy of Sciences, Fuzhou, Fujian 350002, P. R. China*

<sup>3</sup>*Bragg Institute, ANSTO, Locked Bag 2001, Kirrawee DC NSW 2232, Australia*

(Dated: March 28, 2016)

The magnetic structure of the spin-chain antiferromagnet  $\text{SrCo}_2\text{V}_2\text{O}_8$  is determined by single-crystal neutron diffraction experiment. The system undergoes magnetic long range order below  $T_N = 4.96$  K. The moment of  $2.16\mu_B$  per Co at 1.6 K in the screw chain running along the  $c$  axis alternates in the  $c$ -axis. The moments of neighboring screw chains are arranged antiferromagnetically along one in-plane axis and ferromagnetically along the other in-plane axis. This magnetic configuration breaks the 4-fold symmetry of the tetragonal crystal structure and leads to two equally populated magnetic twins with antiferromagnetic vector in the  $a$  or  $b$  axis. The very similar magnetic state to the isostructural  $\text{BaCo}_2\text{V}_2\text{O}_8$  warrants  $\text{SrCo}_2\text{V}_2\text{O}_8$  another interesting half-integer spin-chain antiferromagnet for investigation on quantum antiferromagnetism.

PACS numbers: 75.10.Pq, 75.25.+z, 75.40.Cx, 75.30.Kz

Study on quasi-one-dimensional antiferromagnetic materials in recent decades has revealed interesting quantum magnetic effects which are absent in three-dimensional classical antiferromagnets. While whether the spin is an integer or half-integer would have made no difference in the classical magnetic theory, drastically different physics phenomena have been predicted [1] and demonstrated between the spin  $S = 1$  systems [2–6] and the  $S = \frac{1}{2}$  systems [7–11]. In addition to chain compounds, magnetic moments forming a ladder constitute another important geometric system in investigation on quasi-one-dimensional quantum antiferromagnetism with the competition between the intra and inter-chain exchange interactions as an additional tuning parameter [12–15]. More recently a series of quasi-one-dimensional spin systems built from a screw chain structure have been realized in transition metal vanadates  $AM_2V_2O_8$ , where  $A = \text{Ba}, \text{Sr}, \text{or Pb}$  and  $M = \text{Cu}, \text{Co}, \text{or Ni}$  [16–19]. Remarkably, a quantum phase transition to the Tomonaga-Luttinger liquid has been induced by an external magnetic field in  $\text{BaCo}_2\text{V}_2\text{O}_8$  [20–27].

The magnetic structure of  $\text{BaCo}_2\text{V}_2\text{O}_8$  at the zero magnetic field was first investigated by neutron powder diffraction experiments [23] and completely determined by neutron single-crystal diffraction experiments [24]. The direct measurements of the antiferromagnetic structure and its evolution in magnetic field by neutron diffraction experiments have provided the valuable evidences to compare with theoretical prediction of the novel quantum phenomena in half-integer spin chains [20–24]. For the isostructural  $\text{SrCo}_2\text{V}_2\text{O}_8$ , heat capacity and magnetic susceptibility measurements also indicate a magnetic transition at  $T_N \sim 5$  K [28, 29]. An additional magnetic transition to a canted antiferromagnetic structure at  $\sim 3$  K was reported in one of the studies [28],

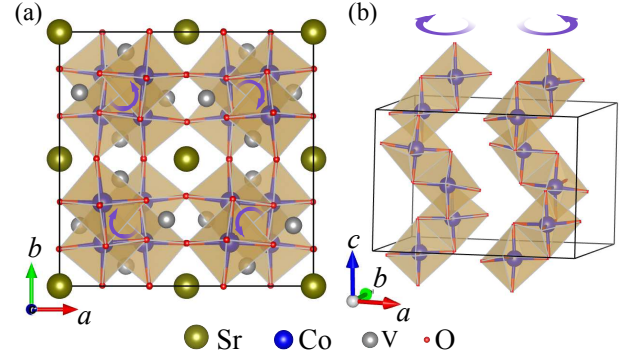


FIG. 1. (color online). Crystal structure of  $\text{SrCo}_2\text{V}_2\text{O}_8$ . (a) Projection to the  $(0,0,1)$  basal plane in the unit cell. (b) The magnetic chains are formed by edge sharing  $\text{CoO}_6$  octahedra. Only two chains with  $0 \leq x \leq 1$  and  $0 \leq y \leq 0.5$  are presented here. The arrows indicate the sense of rotation of the screw chains on increasing  $z$ .

which was different from the case for  $\text{BaCo}_2\text{V}_2\text{O}_8$ . A direct determination of the magnetic configuration by neutron diffraction is called for. In this single-crystal neutron diffraction study of  $\text{SrCo}_2\text{V}_2\text{O}_8$ , we observed only one antiferromagnetic phase transition at  $T_N = 4.96$  K. No anomaly in nuclear or magnetic Bragg peak intensity can be detected around 3 K. The magnetic structure of  $\text{SrCo}_2\text{V}_2\text{O}_8$  is found to be the same as that of  $\text{BaCo}_2\text{V}_2\text{O}_8$  reported previously [24]. The magnetic moment  $2.16(1)\mu_B$  per  $\text{Co}^{2+}$  ion in  $\text{SrCo}_2\text{V}_2\text{O}_8$  is also very close to that of  $\text{BaCo}_2\text{V}_2\text{O}_8$ . Therefore,  $\text{SrCo}_2\text{V}_2\text{O}_8$  can be another candidate of the vanadate series  $AM_2V_2O_8$  for investigation on quasi-one-dimensional quantum antiferromagnetism.

The single crystal sample of  $\text{SrCo}_2\text{V}_2\text{O}_8$  used in this study was grown by spontaneous nucleation method [18]

with dimensions  $\sim 7 \times 7 \times 7 \text{ mm}^3$ . Neutron scattering experiments were performed using the thermal triple-axis spectrometer Taipan at ANSTO [30]. The horizontal collimations were open-40'-40'-open. Neutrons with incident energy  $E = 14.7 \text{ meV}$  were selected using the  $(0, 0, 2)$  reflection of a pyrolytic graphite (PG) monochromator. PG filters were used to remove higher-order neutrons from the neutron beam. The temperature of the sample was regulated by the ILL Orange Cryostat in a temperature range from 1.5 K to 300 K.

$\text{SrCo}_2\text{V}_2\text{O}_8$  crystallizes in the tetragonal  $\text{SrNi}_2(\text{AsO}_4)_2$  structure (space group No. 110,  $I4_1cd$ ) [31], with lattice parameters  $a = 12.267(1) \text{ \AA}$  and  $c = 8.424(1) \text{ \AA}$  at room temperature. In a structural unit cell, the magnetic ions  $\text{Co}^{2+}$  in the edge-shared  $\text{CoO}_6$  octahedra form screw chains along the  $c$ -axis (Fig. 1). The screw chains are well separated by non-magnetic  $\text{VO}_4$  tetrahedra and  $\text{Sr}^{2+}$  ions, resulting in quasi-one-dimensional magnetic chains.

We aligned the  $\text{SrCo}_2\text{V}_2\text{O}_8$  crystal sample to the  $(h0l)$  scattering plane. In the scattering plane, nuclear Bragg peaks were observed at  $h = \text{even}$  and  $l = \text{even}$  positions, which is consistent with the selection rule of the  $I4_1cd$  space group. Below 5 K a new set of magnetic peaks show up at  $h + l = \text{odd}$  positions which are shifted from the nuclear Bragg peaks by the  $\mathbf{Q}_{AF} = (1, 0, 0)$  magnetic wave vector. This situation facilitates the collection and measurements of the separated Bragg peaks of crystalline and magnetic origins.

To investigate the magnetic phase transitions, we measured the temperature dependence of magnetic Bragg reflection  $(-2, 0, -1)$  from 1.6 K to 8.4 K. It clearly illustrates the emergence of new peaks below the magnetic transition. The integrated intensities are fitted to the function  $I = I_0 + A(1 - \frac{T}{T_N})^{2\beta}$  to obtain the critical temperature  $T_N = 4.96(1) \text{ K}$ . It is consistent with the  $\sim 5 \text{ K}$  magnetic transition reported in bulk measurement [28, 29]. The rocking scan in the inset of Fig. 2 has resolution limited peak width and shows no change with temperature. It indicates the long-range nature of the magnetic ordering.

In addition to the 5 K transition, He *et al.* reported a second anomaly at  $\sim 3 \text{ K}$  which is attributed to a transition to a canted antiferromagnetic state in their dynamic magnetic susceptibility work [28]. On the other hand, Lejay *et al.* found no such transition [29]. To check the existence of the possible additional transition, we measured a selected set of structural and magnetic Bragg reflections in more than three quadrants of the scattering plane at 1.6 K and 4 K. The integrated intensities of the nuclear reflections at 1.6 K and 4 K don't yield any observable ferromagnetic signal. There is no anomaly either on antiferromagnetic reflections around 3 K. Therefore, our data do not detect the additional transition.

The propagation vector of the magnetic structure  $\mathbf{Q}_{AF} = (1, 0, 0)$  of  $\text{SrCo}_2\text{V}_2\text{O}_8$  is the same as that of

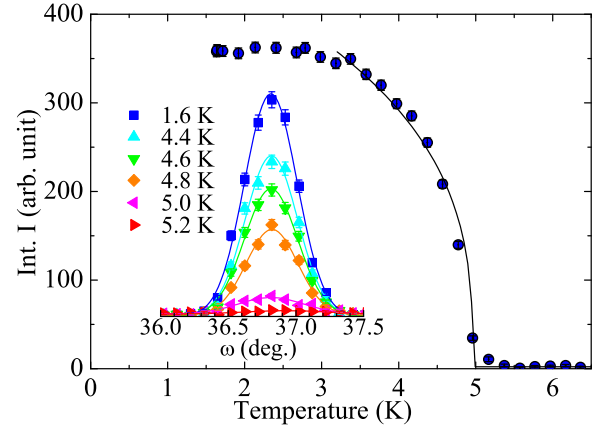


FIG. 2. (color online). Temperature dependence of the  $(-2, 0, -1)$  magnetic peak intensity. The solid circles are experimental data, and the solid line is a fit of the experimental data by the function described in the main text. Inset: Rocking scans of  $(-2, 0, -1)$  Bragg reflection, with increasing temperatures, at 1.6, 4.4, 4.6, 4.8, 5.0 and 5.2 K, respectively.

$\text{BaCo}_2\text{V}_2\text{O}_8$ . In  $\text{BaCo}_2\text{V}_2\text{O}_8$ , the spins of  $\text{Co}^{2+}$  are aligned antiferromagnetically along the screw chains, but at a give basal plane they form antiferromagnetic (or ferromagnetic) alignment along the  $a$  (or  $b$ ) axis [24]. This spin configuration is no longer invariant under the symmetry operator  $4_1$  screw axis of the paramagnetic space group  $I4_1cd$ . Two magnetic domains are thus expected with antiferromagnetic lines formed along either  $a$  or  $b$  axis, as illustrated in Fig. 3 (a) and (b) respectively.

The magnetic neutron scattering cross section [32] of  $\text{SrCo}_2\text{V}_2\text{O}_8$  is described by

$$\sigma(\mathbf{q}) = \left(\frac{\gamma r_0}{2}\right)^2 N_m \frac{(2\pi)^3}{v_m} \langle M \rangle^2 |f(q)|^2 |\mathcal{F}|^2 (1 - (\hat{\mathbf{q}} \cdot \hat{\mathbf{s}})^2), \quad (1)$$

where  $(\frac{\gamma r_0}{2})^2 = 0.07265 \text{ barn}/\mu_B^2$ ,  $N_m$  is the number of magnetic unit cells in the sample,  $v_m$  is the volume of magnetic unit cell,  $M$  is the staggered moment of the  $\text{Co}^{2+}$  ion,  $f(q)$  is the magnetic form factor of the  $\text{Co}^{2+}$ ,  $\hat{\mathbf{q}}$  the unit vector of  $\mathbf{q}$ ,  $\hat{\mathbf{s}}$  the unit vector of the staggered moment, and  $\mathcal{F}$  the magnetic structure factor per unit cell. Using  $(x, y, z)$  as the fractional coordination of the Co atom in the unit cell, and  $(hkl)$  Miller indices of neutron scattering vector  $\mathbf{q}$ , the squared magnetic structure factor  $|\mathcal{F}(\mathbf{q})|^2$  of the antiferromagnetic model shown in Fig. 3(a) is

$$|\mathcal{F}(\mathbf{q})|^2 = 64 \{ \sin(2\pi hx) - \sin(2\pi hy) \}^2 \quad (2)$$

for  $h = 2n + 1, l = 4n$ , and

$$|\mathcal{F}(\mathbf{q})|^2 = 64 \{ \sin(2\pi hx) + \sin(2\pi hy) \}^2 \quad (3)$$

for  $h = 2n + 1, l = 4n + 2$ . Namely, for domain 1, magnetic signals only appear on positions of  $h = \text{odd}$  and  $l = \text{even}$  in the  $(h0l)$  scattering plane. For domain 2 in Fig. 3(b),

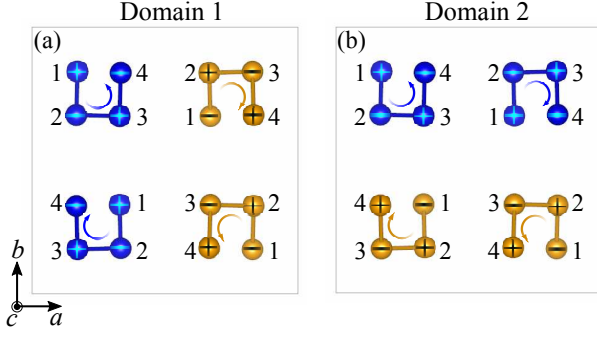


FIG. 3. (color online). Two magnetic domains of  $\text{SrCo}_2\text{V}_2\text{O}_8$  viewed in  $c$  axis. Only intrachain bonded Co atoms are presented, with their sense of rotation marked by screw arrows. The  $c$ -axis fractional coordinates are  $z$ ,  $z+1/4$ ,  $z+1/2$ ,  $z+3/4$  respectively for Co with '1', '2', '3', '4' labels. Spin directions parallel or antiparallel to the  $c$  axis are marked by '+' and '-' signs. The same (blue and yellow) colors present ferromagnetic arrangement in basal plane.

the magnetic peaks only present when  $h = \text{even}$  and  $l = \text{odd}$ , and

$$|\mathcal{F}(\mathbf{q})|^2 = 64\{\sin^2(2\pi hx) + \sin^2(2\pi hy)\} \quad (4)$$

for  $h = 2n$ ,  $l = 2n + 1$ .

The measured magnetic cross-section deduced from the integrated intensity of the rocking scans by  $\sigma(\mathbf{q}) = I \sin(2\theta)$  and normalized by nuclear Bragg peaks is shown in Fig. 4(a). The blue and red symbols denote Bragg intensities from the domain 1 and 2 shown in Fig. 3, respectively. The experimental data agree well with the intensities calculated with the same magnetic structure of  $\text{BaCo}_2\text{V}_2\text{O}_8$  [24] but of a staggered magnetic moment  $2.16(1)\mu_B$  per Co, see Fig. 4(b). The relative intensities of the blue and red Bragg peaks lead to the domain population 49.9(1)% for domain 1 and 50.1(1)% for domain 2 in the least squared fit. Therefore, the two domains have essentially the equal population. After we finished our work, we noticed a neutron powder diffraction work on magnetic structure of  $\text{SrCo}_2\text{V}_2\text{O}_8$  [33]. Both  $T_N = 5.21(3)$  and  $M = 2.25(5)\mu_B/\text{Co}$  are slightly larger than our values. While the same magnetic structure was reported by Bera et al., the domain population can be measured only in a single-crystal diffraction experiment and the domain information is important in achieving the realistic refinement result, as pointed out by Canévet *et al.* [24].

The magnetic structure of  $\text{SrCo}_2\text{V}_2\text{O}_8$  is identical to that of the isostructural  $\text{BaCo}_2\text{V}_2\text{O}_8$ . Only the Co moment  $2.16(1)\mu_B$  is slightly smaller than  $2.267(3)\mu_B$  reported for  $\text{BaCo}_2\text{V}_2\text{O}_8$  [24]. Our result thus explains the similar macroscopic properties observed in bulk measurements: Both  $\text{SrCo}_2\text{V}_2\text{O}_8$  and  $\text{BaCo}_2\text{V}_2\text{O}_8$  show  $\lambda$ -shape anomalies in heat capacity measurements at  $T_N \sim 5\text{K}$  at zero magnetic field. The antiferromagnetic order is

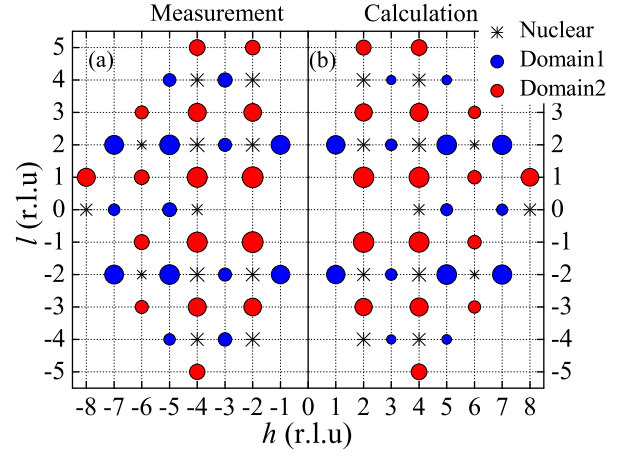


FIG. 4. (color online). Scattering pattern in reciprocal lattice of  $(h0l)$  plane. (a) Measured Bragg peaks at 1.6 K. (b) Calculated results. Asterisks mark the structural Bragg peaks. The filled blue circles are magnetic peaks of domain 1, and filled red circles are magnetic peaks of domain 2. The logarithmic scale is used for the magnetic intensities that are illustrated by the size of symbols.

suppressed by magnetic field in similar manners for both compounds, with the critical field smaller for  $H \parallel c$  than  $H \perp c$  [17, 18, 29, 34]. The same in-plane anisotropy between  $H \parallel (110)$  and  $(100)$  was also recently revealed [34–36]. In the substitution study, all the key features are preserved in  $\text{Ba}_{1-x}\text{Sr}_x\text{Co}_2\text{V}_2\text{O}_8$  in thermal expansion and magnetostriction measurements [34].

As a realization of the one-dimensional XXZ half-integer spin chain model,  $\text{BaCo}_2\text{V}_2\text{O}_8$  has shown the predicted magnetic field-induced quantum spin liquid behavior [20–24]. Although such field induced phenomena has not been confirmed in  $\text{SrCo}_2\text{V}_2\text{O}_8$ , the same zero-field magnetic state suggests that  $\text{SrCo}_2\text{V}_2\text{O}_8$  could be another interesting material to explore the novel quantum spin properties. Recent terahertz spectroscopy experiments show that  $\text{SrCo}_2\text{V}_2\text{O}_8$  is less anisotropic than  $\text{BaCo}_2\text{V}_2\text{O}_8$  with the anisotropy parameter  $\epsilon \approx 0.73$  comparing to  $\epsilon \approx 0.46$  for the latter, with  $\epsilon = 1$  corresponding to the isotropic Heisenberg limit [37, 38]. Therefore,  $\text{SrCo}_2\text{V}_2\text{O}_8$  from the transition metal vanadates series  $AM_2V_2O_8$  provides an interesting tuning parameter in the anisotropy parameter. Additional tuning parameter, such as that in the spin ladder compounds [12–15], would enrich study on quasi-one-dimensional quantum antiferromagnetism.

In conclusion, the magnetic structure of  $\text{SrCo}_2\text{V}_2\text{O}_8$  is determined in our neutron single-crystal diffraction study as the same as that of  $\text{BaCo}_2\text{V}_2\text{O}_8$  [23]. The magnetic moment of the  $\text{Co}^{2+}$  ions is  $2.16(1)\mu_B/\text{Co}$  at 1.6 K and the Néel temperature is  $4.96(1)\text{K}$ . The antiferromagnetic structure breaks the four-fold in-plane symmetry and the resulting two magnetic domains have the iden-

tical population. We do not observe the 3 K canting transition, thus  $\text{SrCo}_2\text{V}_2\text{O}_8$  and  $\text{BaCo}_2\text{V}_2\text{O}_8$  share the same zero field magnetic state. With almost identical magnetic state but less magnetic anisotropy,  $\text{SrCo}_2\text{V}_2\text{O}_8$  could be a worthy addition to  $\text{BaCo}_2\text{V}_2\text{O}_8$  in investigation on spin-chain quantum antiferromagnetism.

The work at RUC and FIRSM was supported by National Basic Research Program of China (Grant Nos. 2012CB921700 and 2011CBA00112) and the National Natural Science Foundation of China (Grant Nos. 11034012 and 11190024).

---

\* wbao@ruc.edu.cn

- [1] F. D. M. Haldane, Phys. Rev. Lett. **45**, 1358 (1980).
- [2] M. Steiner, K. Kakurai, J. K. Kjems, D. Petitgrand, and R. Pynn, J. Appl. Phys. **61**, 3953 (1987).
- [3] W. J. L. Buyers, R. M. Morra, R. L. Armstrong, M. J. Hogan, P. Gerlach, and K. Hirakawa, Phys. Rev. Lett. **56**, 371 (1986).
- [4] S. Ma, C. Broholm, D. H. Reich, B. J. Sternlieb, and R. W. Erwin, Phys. Rev. Lett. **69**, 3571 (1992).
- [5] L. P. Regnault, I. Zaliznyak, J. P. Renard, and C. Vetter, Phys. Rev. B **50**, 9174 (1994).
- [6] S. Suh, K. A. Al-Hassanieh, E. C. Samulon, I. R. Fisher, S. E. Brown, and C. D. Batista, Phys. Rev. B **84**, 054413 (2011).
- [7] D. A. Tennant, R. A. Cowley, S. E. Nagler, and A. M. Tsvelik, Phys. Rev. B **52**, 13368 (1995).
- [8] D. C. Dender, P. R. Hammar, D. H. Reich, C. Broholm, and G. Aeppli, Phys. Rev. Lett. **79**, 1750 (1997).
- [9] T. Giamarchi, C. Rüegg, and O. Tchernyshyov, Nature Physics **4**, 198 (2008).
- [10] B. S. Conner, H. D. Zhou, Y. J. Jo, L. Balicas, C. R. Wiebe, J. P. Carlo, Y. J. Uemura, A. A. Aczel, T. J. Williams, and G. M. Luke, Phys. Rev. B **81**, 132401 (2010).
- [11] I. A. Zaliznyak, S.-H. Lee, and S. V. Petrov, Phys. Rev. Lett. **87**, 017202 (2001).
- [12] M. Klanjšek, H. Mayaffre, C. Berthier, M. Horvatić, B. Chiari, O. Piovesana, P. Bouillot, C. Kollath, E. Orignac, R. Citro, and T. Giamarchi, Phys. Rev. Lett. **101**, 137207 (2008).
- [13] C. Rüegg, K. Kiefer, B. Thielemann, D. F. McMorro, V. Zapf, B. Normand, M. B. Zvonarev, P. Bouillot, C. Kollath, T. Giamarchi, S. Capponi, D. Poilblanc, D. Biner, and K. W. Krämer, Phys. Rev. Lett. **101**, 247202 (2008).
- [14] M. Jeong, H. Mayaffre, C. Berthier, D. Schmidiger, A. Zheludev, and M. Horvatić, Phys. Rev. Lett. **111**, 106404 (2013).
- [15] B. Lake, D. A. Tennant, J.-S. Caux, T. Barthel, U. Schollwöck, S. E. Nagler, and C. D. Frost, Phys. Rev. Lett. **111**, 137205 (2013).
- [16] Z. He, T. Kyômen, and M. Itoh, J. Cryst. Growth **274**, 486 (2005).
- [17] Z. He, D. Fu, T. Kyômen, T. Taniyama, and M. Itoh, Chem. Mater. **17**, 2924 (2005).
- [18] Z. He, T. Taniyama, and M. Itoh, J. Cryst. Growth **293**, 458 (2006).
- [19] Z. He, Y. Ueda, and M. Itoh, J. Solid State Chem. **180**, 1770 (2007).
- [20] S. Kimura, T. Takeuchi, K. Okunishi, M. Hagiwara, Z. He, K. Kindo, T. Taniyama, and M. Itoh, Phys. Rev. Lett. **100**, 057202 (2008).
- [21] K. Okunishi and T. Suzuki, Phys. Rev. B **76**, 224411 (2007).
- [22] S. Kimura, M. Matsuda, T. Masuda, S. Hondo, K. Kaneko, N. Metoki, M. Hagiwara, T. Takeuchi, K. Okunishi, Z. He, K. Kindo, T. Taniyama, and M. Itoh, Phys. Rev. Lett. **101**, 207201 (2008).
- [23] Y. Kawasaki, J. L. Gavilano, L. Keller, J. Schefer, N. B. Christensen, A. Amato, T. Ohno, Y. Kishimoto, Z. He, Y. Ueda, and M. Itoh, Phys. Rev. B **83**, 064421 (2011).
- [24] E. Canévet, B. Grenier, M. Klanjšek, C. Berthier, M. Horvatić, V. Simonet, and P. Lejay, Phys. Rev. B **87**, 054408 (2013).
- [25] M. Klanjšek, M. Horvatić, S. Krämer, S. Mukhopadhyay, H. Mayaffre, C. Berthier, E. Canévet, B. Grenier, P. Lejay, and E. Orignac, Phys. Rev. B **92**, 060408 (2015).
- [26] B. Grenier, V. Simonet, B. Canals, P. Lejay, M. Klanjšek, M. Horvatić, and C. Berthier, Phys. Rev. B **92**, 134416 (2015).
- [27] B. Grenier, S. Petit, V. Simonet, E. Canévet, L.-P. Regnault, S. Raymond, B. Canals, C. Berthier, and P. Lejay, Phys. Rev. Lett. **114**, 017201 (2015).
- [28] Z. He, T. Taniyama, M. Itoh, J.-I. Yamaura, and Y. Ueda, Solid State Commun. **141**, 667 (2007).
- [29] P. Lejay, E. Canévet, S. Srivastava, B. Grenier, M. Klanjšek, and C. Berthier, J. Cryst. Growth **317**, 128 (2011).
- [30] S. A. Danilkin, G. Horton, R. Moore, G. Braoudakis, and M. Hagen, J. Neutron Res. **15**, 55 (2007).
- [31] D. Osterloh and H. Mueller Buschbaum, Z. Naturforsch. B Chem. Sci. **49**, 923 (1994).
- [32] G. L. Squires, *Introduction to the Theory of Thermal Neutron Scattering* (Cambridge University Press, Cambridge, 2012).
- [33] A. K. Bera, B. Lake, W.-D. Stein, and S. Zander, Phys. Rev. B **89**, 094402 (2014).
- [34] S. K. Niesen, O. Breunig, S. Salm, M. Seher, M. Valldor, P. Warzanowski, and T. Lorenz, Phys. Rev. B **90**, 104419 (2014).
- [35] S. Kimura, K. Okunishi, M. Hagiwara, K. Kindo, Z. He, T. Taniyama, M. Itoh, K. Koyama, and K. Watanabe, J. Phys. Soc. Jpn. **82**, 033706 (2013).
- [36] S. K. Niesen, G. Kolland, M. Seher, O. Breunig, M. Valldor, M. Braden, B. Grenier, and T. Lorenz, Phys. Rev. B **87**, 224413 (2013).
- [37] Z. Wang, M. Schmidt, A. K. Bera, A. T. M. N. Islam, B. Lake, A. Loidl, and J. Deisenhofer, Phys. Rev. B **91**, 140404 (2015).
- [38] S. Kimura, H. Yashiro, M. Hagiwara, K. Okunishi, K. Kindo, Z. He, T. Taniyama, and M. Itoh, J. Phys.: Conf. Ser. **51**, 99 (2006).